Imaging of the mouse lung with scanning laser optical tomography (SLOT)

Marko Heidrich[1*], Manuela Kellner[2*], Rebecca Beigel[2,3], Raoul-Amadeus Lorbeer[1], Lars Knudsen[2,4], Alexander Heisterkamp[3,4,5], Tammo Ripken[1,3], Matthias Ochs[2,3,4], Mark Philipp Kühnel[2**], Heiko Meyer[1,3,6**]

[1]Biomedical Optics Department, Laser Zentrum Hannover e.V., Hannover, Germany;
[2]Institute of Functional and Applied Anatomy, Hannover Medical School, Hannover, Germany;
[3]REBIRTH Cluster of Excellence, Hannover, Germany;
[4]Member of the German Center for Lung Research (DZL), Hannover, Germany;
[5]Institute of Applied Optics, Friedrich-Schiller-University Jena, Jena, Germany;
[6]Department of Cardiothoracic, Transplantation and Vascular Surgery (HTTG), Hannover Medical School, Hannover, Germany;

ABSTRACT

New optical techniques have the potential to fill the gap between radiological and microscopic approaches to assess the lung's internal structure. Since its quantitative assessment requires unbiased sampling and measurement principles, imaging of the whole lung with sufficient resolution for visualizing details is important. To address this request, we applied scanning laser optical tomography (SLOT) for the three dimensional imaging of mouse lung *ex vivo*. SLOT is a highly efficient fluorescence and transmission microscopy technique allowing for 3D imaging of specimen of sizes up to several millimeters. Previously fixed lung lobes and whole lungs were optically cleared and subsequently imaged with SLOT while making use of intrinsic contrast mechanisms like absorption and autofluorescence. Imaging of airways, blood vessels and parenchyma is demonstrated. Volumetric SLOT datasets of the lung's internal structure can be analyzed in any preferred planar orientation. Moreover, the sample preparation preserves microscopic structure of the lung and allows for subsequent correlative histologic studies. In summary, SLOT is a useful technique to visualize and survey the internal structure of mouse lung at different scales and with various contrast mechanisms. Potential applications of SLOT in lung research are e.g. quantitative phenotype analysis of mouse models of human lung disease in combination with stereological methods.

Keywords: 3D fluorescence microscopy, optical projection tomography, acini, alveoli, airways, blood vessels

1. INTRODUCTION

Radiological methods like X-ray based computed tomography (CT) or magnetic resonance imaging (MRI) proved to be useful for assessing the lung's internal structure.[1] These techniques are capable of imaging the whole organ *in vivo* but are limited in resolution. This disadvantage can be overcome by the application of standard wide field or electron microscopy[1–3] which provide high resolution but are usually based on sections from samples after fixation, embedding and sectioning. Moreover, the histologic procedure tends to be time-consuming and does not allow the three dimensional analysis of the internal lung structure.

Advanced optical imaging techniques like confocal fluorescence endomicroscopy,[4] multiphoton microscopy (MPM),[5–7] fluorescence molecular tomography (FMT)[8,9] and optical coherence tomography (OCT)[10–15] overcome these constraints and may fill the imaging gap, in particular in experimental studies. These techniques do

Further author information: *These authors contributed equally to this study and share first authorship. **These authors contributed equally to this study and share senior authorship.
Send correspondence to Marko Heidrich: m.heidrich@lzh.de, Telephone: 49 511 2788 222

Photonic Therapeutics and Diagnostics IX, edited by Nikiforos Kollias, et al., Proc. of SPIE Vol. 8565, 856535 · © 2013 SPIE · CCC code: 1605-7422/13/$18 · doi: 10.1117/12.2003955

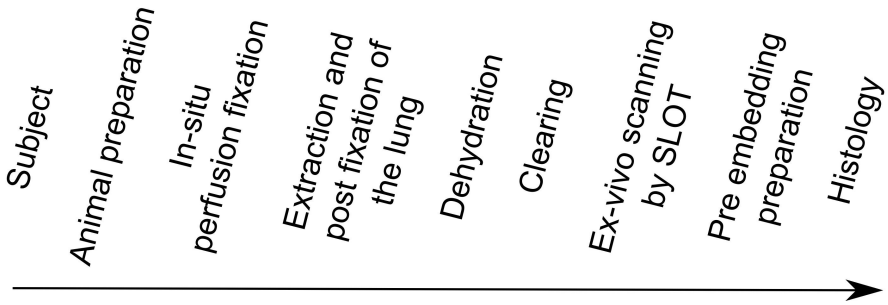

Figure 1. Workflow chart of the sample preparation. (See[22] for details.)

not require tissue fixation and endoscopic applications allow for observation of bronchial epithelial and subepithelial regions *in vivo*. However, the strong light scattering of native i.e. optically uncleared tissue restricts the penetration depth making it challenging to image larger samples or whole organs at high resolution.

Since the quantitative assessment of the lung requires unbiased sampling and measurement principles,[16] techniques for lung imaging should permit access to the whole lung and provide high optical resolution for the visualization of structural details. Particularly promising in this respect is the recently introduced scanning laser optical tomography (SLOT).[17] SLOT is a highly efficient fluorescence and transmission microscopy technique allowing for 3D imaging of specimen of sizes up to several millimeters. Similary to optical projection tomography (OPT),[18] SLOT can be seen as a light equivalent of X-ray CT. However, SLOT does provide a significantly higher photon collection efficiency and therefore higher sensitivity compared to OPT. Besides the detection of fluorescent markers, SLOT is able to make use of intrinsic contrast mechanisms like autofluorescence, absorption and scattered light[19] which can be detected simultaneously. It needs to be pointed out, that light scattered within the specimen may limit the penetration depth but also provides image information in SLOT.

The application of SLOT presented here focuses on its ability to image the mouse lung at different scales. Thereby, signals of intrinsic contrast mechanisms namely absorption and autofluorescence were utilized in transmission and fluorescence detection mode to visualize structural details within the lung (airways, blood vessels, acini, alveoli).

2. MATERIALS AND METHODS

Mice. C57BL/6 mice were used.[20,21] Animals were housed in an animal facility at Hannover Medical School, with food and water provided *ad libitum*. All animals received humane care in compliance with the "Principles of Laboratory Animal Care" formulated by the National Society for Medical Research and the "Guide for the Care and Use of Laboratory Animals", published by the National Institute of Health (NIH publication 85-23, revised in 1996). The protocol is in compliance with the Protection of Animals Act and approved by the bioethical committee of the district of Lower Saxony.

Lung processing. The workflow and processing steps illustrated in Figure 1 are described in detail elsewhere.[22] Lungs were fixed *in situ* by intravascular perfusion. For subsequent optical clearing of the lungs dehydration was performed in an increasing ethanol series of 30, 50, 70, 90 and 99.8 % ethanol with at least 2 h incubation time per step. Afterwards, lungs were transferred in a mixture of 3 parts methylsalicylic acid (MS) and 2 parts benzyl benzoate (BB) for refractive index matching[23] (corresponding to a refractive index of 1.553). Samples appeared optically clear after 2-3 h and stayed immersed for measurements with SLOT.

SLOT imaging. The SLOT setup is shown in Figure 2. A light source (laser diode, 532 nm, cw, 10mW, not shown here) is coupled into the SLOT setup via single mode fiber (450-600 nm FC/PC Single Mode, Mode Field Diameter 3.5 µm at 515 nm). The beam diameter is adjusted by a 10x motorized zoom lens (1/2" 12-120mm f1.8, computar, CBC (AMERICA) Corp., Commack, NY 11725, USA) to determine the numerical aperture (NA) of the optical system in the illumination path and thereby optical resolution and depth of field. The beam is scanned through a telecentric f-theta lens (80mm, 532nm, Sill Optics GmbH & Co. KG, D-90530 Wendelstein, Germany) by a set of galvanometer-scanning mirrors (ProSeries II Scan Head - 14 mm, Cambridge Technology, Inc., 82152 Planegg, Germany) into a glass cuvette with the specimen immersed in clearing solution. A photodiode (PD)

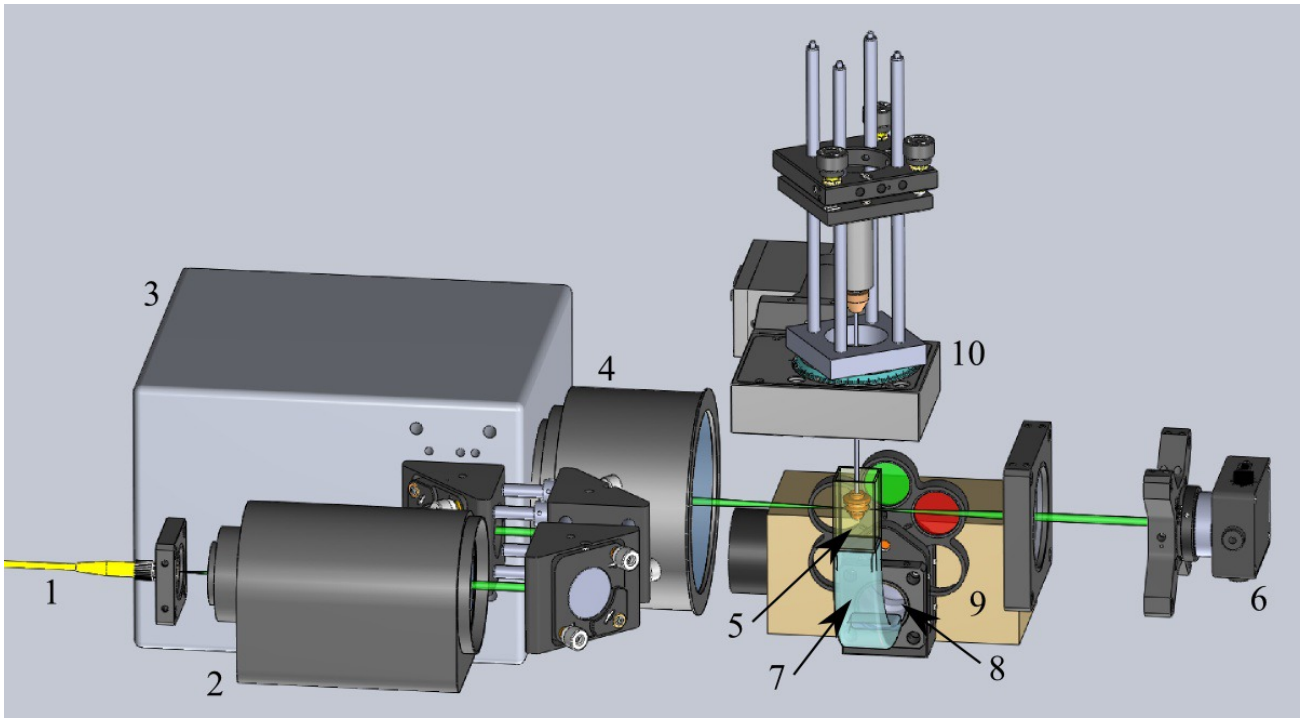

Figure 2. SLOT setup. The laser source (not shown here) is coupled into the setup via single mode fiber (1). The beam diameter is adjusted by a 10x motorized zoom lens (2) to determine the numerical aperture (NA) of the optical system in the illumination path. The laser is scanned (3) through a telecentric f-theta lens (4) into a glass cuvette (5) filled with immersion liquid to acquire projection images of the specimen. Therefore, transmitted light is detected by a photodiode (6, PD) on the optical axis behind the cuvette. Simultaneously, the autofluorescence signal is guided by a fiber bundle (7) below the cuvette, collected by a lens system (8) and detected by a photomultiplier tube (9, PMT). The optical filter blocks the excitation light of the laser source. A rotation stage (10) is used to rotate the specimen within the cuvette.

(PDA36A, Thorlabs, Karlsruhe, Germany) on the optical axis of the system behind the cuvette detects the transmitted laser light to acquire projection images of the extinction. In addition, autofluorescence excited by the 532 nm laser and emitted in the direction of the bottom of the cuvette is detected by a photomultiplier tube (PMT) (R3896, Hamamatsu Photonics K.K., Hamamatsu City, Japan) to obtain projection images of the autofluorescence. Therefore, a fiber bundle guides fluorescence from the bottom of the cuvette to a lens system with an optical band pass filter (FF01-624/40-25, Semrock, Lake Forest, IL) which is used to direct the emitted light onto the PMT and to block scattered laser light. A mechanical rotation stage (M60, Physik Instrumente (PI) GmbH & Co. KG, 76228 Karlsruhe/Palmbach, Germany) rotates the specimen to achieve projection images from multiple viewing angles. The setup allows the simultaneous acquisition of a pair of projection images by using transmitted light (via PD) and autofluorescence (via PMT). Each projection image is formed by scanning 700x700 points through the sample within 2.7 s. By successively capturing projection images and rotating the specimen 360 degrees, a pair of projection image sets is generated, each consisting of 600 images and covering a full revolution (i.e. every 0.6 degrees a projection image pair is captured). Thus, the total time for the acquisition of a full scan is about 27 minutes. To reconstruct a projection image set, custom software is applied performing a filtered back projection algorithm as known from OPT and CT.[24] Thereby a volumetric data stack is created that represents a three-dimensional image of the specimen. All projection data sets and volumetric data stacks were clipped and visualized with the open source software ImageJ.

Light microscopy. For subsequent light microscopic analysis, the cleared accessory lobes were treated with a decreasing acetone series ranging from 100% - 25% acetone in 25% steps for 1 hour each. Samples were then osmicated, immersed in half-saturated aqueous uranyl acetate, dehydrated in acetone and finally embedded in glycol methacrylate (Technovit 8100, Heraeus Kulzer, Wehrheim, Germany). Sections of a thickness of 1.5 µm were cut and stained with toluidine blue for correlative light microscopy.

3. RESULTS

To allow the illumination laser to penetrate the lung tissue without scattering, the lungs were optically cleared by replacing the water with a mixture of MS/BB. Optical clearing of biological samples for conventional light microscopy using MS/BB was established by Spalteholz[23] in 1911.

After imaging with SLOT, the clearing process was reversed via treatment with 100% acetone. Accessory lobes were embedded in glycol methacrylate for histological comparison with lungs that were conventionally embedded for histology.[22]

The optical resolution of SLOT depends on the spatial extent of the investigated sample in beam direction, since the NA of the illumination laser beam has to be adjusted until the specimen is covered by the depth of field.[17] Therefore, imaging the accessory lobe with its thickness of about 2 mm requires an NA of 0.028. This results in a theoretical resolution of 9.3 µm at a laser wavelength of 532 nm which is the theoretical optical resolution for the whole volumetric data stack of the lobe.

Figure 3 A shows a projection image of one of 600 projections generated via transmission of the 532 nm laser through the accessory lobe. Due to high absorption of erythrocytes at 532 nm, the erythrocytes remaining in the blood vessels produce a strong signal drop in the transmission mode. In contrast, blood vessels, which are largely washed out during the fixation procedure, are barely detectable. The corresponding projection generated via detection of autofluorescence is shown in Figure 3 B. Using this contrast mechanism, both the bronchial tree as well as alveolar ducts and alveoli are apparent. While bronchiolar walls stand out via strong autofluorescence, the structure of the acini, alveolar ducts and alveoli, can also be visualized despite their weaker autofluorescence due to the high sensitivity of SLOT. Figure 3 C is an overlay image of the inverted transmission image (Figure 3 A, red) and the autofluorescence image (Figure 3 B, green). It gives a holistic view of the blood vessel (red) and airway (green) structure of the accessory lobe. The projection raw data in Figure 3 demonstrates that the actual resolution is sufficient for visualization of conducting airways and blood vessels in the center of the lobe as well as acinar airways including alveoli in the periphery.

To obtain volumetric data stacks from projection raw data sets, reconstruction via filtered back projection was performed. Thereby stacks of optical slices are generated each slice having a thickness of 6.5 µm (linear voxel size) and allowing the comparison with conventional histology, which is illustrated in Figure 4. It verifies the notion, that the strong autofluorescence originates from the bronchiolar walls (epithelium and sub-epithelial connective tissue), whereas absorption of the 532 nm laser occurs predominantly in blood vessels filled with erythrocytes. However, it should be noted that the fine structure of the parenchyma down to single alveoli can be seen in both in transmission and autofluorescence.

To study the potential of SLOT to image even larger specimen, projection images of a whole mouse lung were acquired. Figure 5 A shows an inverted projection image detected in transmission mode of a whole mouse

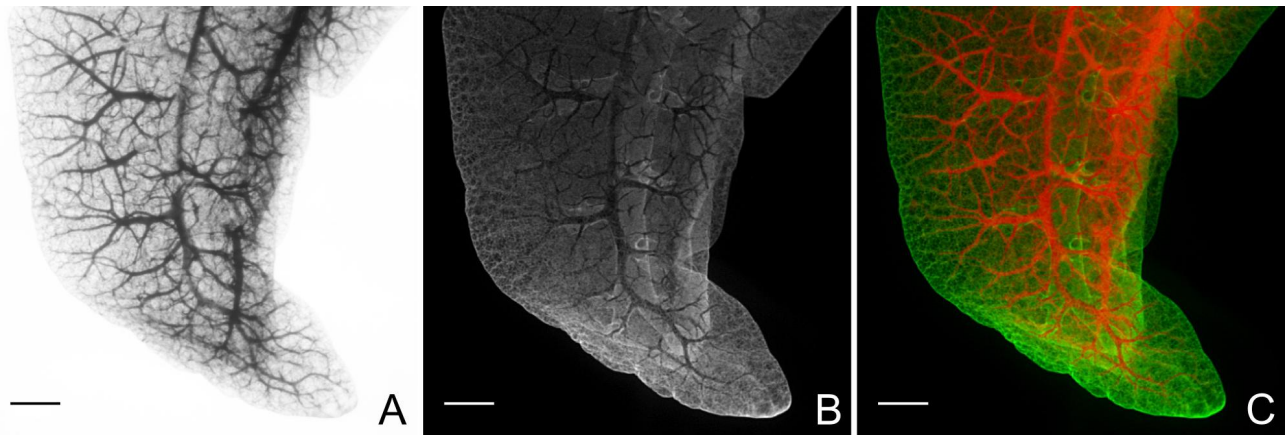

Figure 3. SLOT projection images. A: Transmission image (PD detection) showing blood vessels due to the absorbent properties of the erythrocytes at 532 nm. B: Autofluorescence (PMT detection) image showing airways, acini, alveolar ducts and alveoli. C: Overlay of the autofluorescence in green and the transmission in red. Scale bars are 500 µm.

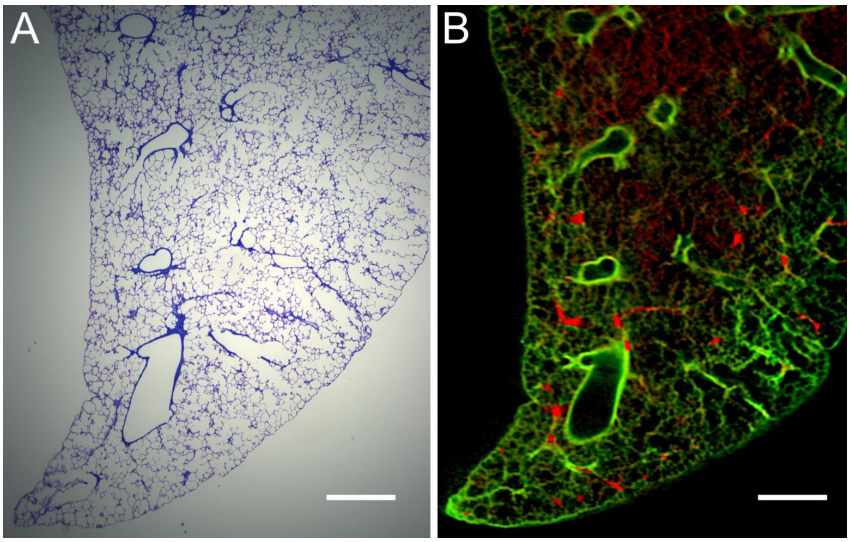

Figure 4. Image correlation of histology and SLOT. Histological section of the accessory lobe by light microscopy (A) and optical slice of nearly the same section obtained by SLOT (B). The overlay of the absorption (red) and the autofluorescence (green) shows similar structures as the histological section. The bronchiolar walls are visualized due to the strong autofluorescence signal of the epithelium and sub-epithelial connective tissue while small blood vessels are visible through the absorbent properties of the erythrocytes. Scale bars are 500 µm.

lung (week 3) illuminated at a wavelength of 532 nm. Since the lung was washed out very thoroughly, almost no blood vessels are visible due to the absence of erythrocytes. A reconstructed optical slice of this projection data set through the whole mouse lung is shown in Figure 5 B. Airways and acini are clearly visible in the outer part of the lung. Due to the thickness of this specimen of about 9.5 mm, an NA of 0.013 is required resulting in a theoretical optical resolution of 20 µm for the whole mouse lung.

4. DISCUSSION

Scanning laser optical tomography (SLOT) is a highly efficient fluorescence and transmission microscopy technique allowing for 3D imaging of specimen of sizes up to several millimeters. Here, SLOT was used as a tool for imaging the mouse lung at different length scales. Whole lung lobes are visualized *ex vivo* with an optical resolution down to the level of alveoli. The acquisition of volumetric data from whole mouse lungs *ex vivo* is demonstrated. Thereby, spatial information is fully preserved allowing the analysis of airways and blood in any preferred orientation.

The physical properties of the intrinsic contrast mechanisms like autofluorescence in lung tissue that can be utilized with SLOT are not fully clear yet and remain to be determined in detail in future studies. A further point that needs to be addressed in this context is the influence of the lung fixation technique, in particular the route of fixation and the chemical composition of the fixative. Also, the visualization of blood vessels depends on the degree to which erythrocytes are flushed out during perfusion. Therefore, depending on the specific purpose of the study, the fixation protocol may have to be adapted accordingly.[25] However, it should be pointed out that specific labeling of target structures with fluorescent markers are possible in SLOT[17] just as OPT.[26]

In comparison to other imaging modalities, SLOT is an efficient and convenient technique which enables to record both fluorescent and non-fluorescent volumetric data from intact samples of a size of several millimeters.[17,19] Besides whole lobes from mouse lungs, tissue samples of similar size from large animal or human lungs can be analyzed with the same optical resolution. Moreover, due to the large field of view provided by the f-theta lens, even larger specimen of up to 40 mm may be imaged with SLOT. One limitation of this approach is that the samples need to be transparent, i.e. suitable clearing protocols have to be employed. The lung with its low tissue volume fraction and large connected inner spaces is particularly suited for optical clearing. However, in

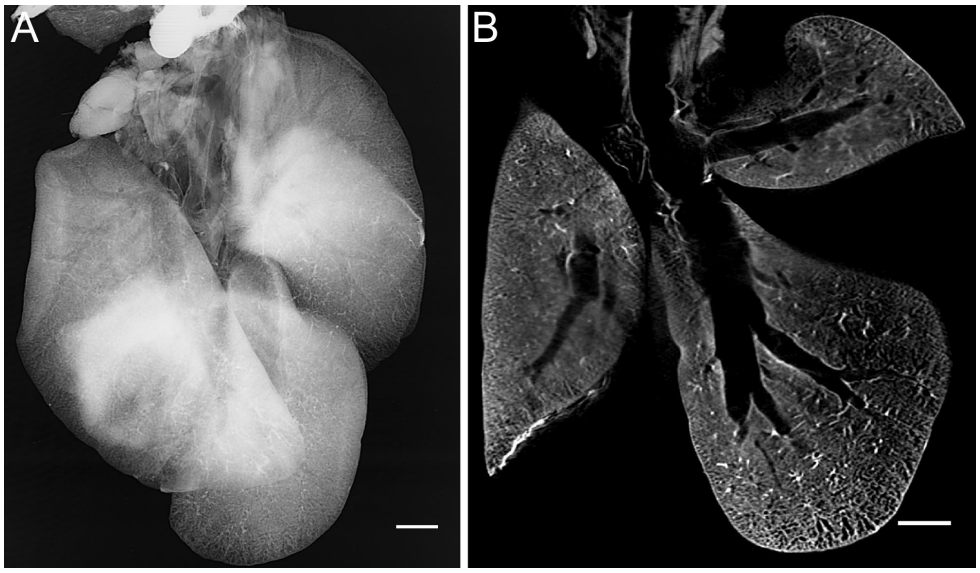

Figure 5. Imaging a whole mouse lung with SLOT. A: Inverted projection image detected in transmission mode (with PD). B: Optical slice through the related volumetric data stack. Scale bars are 1 mm.

very dense and large organs clearing can be challenging. Lung tissue can easily be cleared for SLOT while still maintaining tissue fine structure for subsequent histologic analysis.

Potential applications of SLOT in lung research are e.g. quantitative phenotype analysis of mouse models of human lung disease. Here, SLOT can be used in combination with stereological methods.[16,22,27]

In summary, we were able to show that scanning laser optical tomography (SLOT) is a useful technique to study the internal structure of the entire mouse lung. Our ongoing studies focus on obtaining quantitative information by combining SLOT and stereology, in particular in mouse models of lung injury and disease.

ACKNOWLEDGMENTS

This work was supported by the REBIRTH Cluster of Excellence and the German Center for Lung Research (DZL). For excellent technical support, we thank S. Kuhlmann (Institute of Functional and Applied Anatomy, Hannover Medical School, Hannover, Germany). Furthermore, we would like to thank the program developers of the open source software ImageJ (rsbweb.nih.gov/ij/).

REFERENCES

[1] Brown, R. H., Irvin, C. G., Allen, G. B., Shapiro, S. D., Martin, W. J., Kolb, M. R. J., Hyde, D. M., Nieman, G. F., Cody, D. D., Ishii, M., Kadlecek, S. J., Driehuys, B., Rizi, R. R., Wu, A. M., Weber, W. a., and Stout, D. B., "An official ATS conference proceedings: advances in small-animal imaging application to lung pathophysiology.," *Proceedings of the American Thoracic Society* **5**, 591–600 (July 2008).

[2] Schraufnagel, D. E., [*Electron microscopy of the lung*], M. Dekker, New York (1990).

[3] Schuster, D. P. and Blackwell, T., [*Molecular imaging of the lungs*], Taylor & Francis, Boca Raton (2005).

[4] Thiberville, L., Moreno-Swirc, S., Vercauteren, T., Peltier, E., Cavé, C., and Bourg Heckly, G., "In vivo imaging of the bronchial wall microstructure using fibered confocal fluorescence microscopy.," *American journal of respiratory and critical care medicine* **175**, 22–31 (Jan. 2007).

[5] Abraham, T., Wadsworth, S., Carthy, J. M., Pechkovsky, D. V., and McManus, B., "Minimally invasive imaging method based on second harmonic generation and multiphoton excitation fluorescence in translational respiratory research," *Respirology* **16**, 22–33 (Jan. 2011).

[6] Parra, S. G., Chia, T. H., Zinter, J. P., and Levene, M. J., "Multiphoton microscopy of cleared mouse organs.," *Journal of biomedical optics* **15**(3), 036017 (2010).

[7] Pena, A., Fabre, A., Débarre, D., Marchal-Somme, J., Crestani, B., Martin, J., Beaurepaire, E., and Schanne-Klein, M.-C., "Three-Dimensional Investigation and Scoring of Extracellular Matrix Remodeling During Lung Fibrosis Using Multiphoton Microscopy," *Microscopy research and technique* **70**(2), 162–170 (2007).

[8] Ntziachristos, V., Ripoll, J., Wang, L. V., and Weissleder, R., "Looking and listening to light: the evolution of whole-body photonic imaging," *Nature biotechnology* **23**, 313–20 (Mar. 2005).

[9] Haller, J., Hyde, D., Deliolanis, N., Kleine, R. d., Niedre, M., and Ntziachristos, V., "Visualization of pulmonary inflammation using noninvasive fluorescence molecular imaging," *Journal of Applied Physiology* **104**, 795–802 (Jan. 2008).

[10] Coxson, H. O. and Lam, S., "Quantitative assessment of the airway wall using computed tomography and optical coherence tomography.," *Proceedings of the American Thoracic Society* **6**, 439–443 (Aug. 2009).

[11] Meissner, S., Knels, L., Schnabel, C., Koch, T., and Koch, E., "Three-dimensional Fourier domain optical coherence tomography in vivo imaging of alveolar tissue in the intact thorax using the parietal pleura as a window.," *Journal of biomedical optics* **15**(1), 016030 (2010).

[12] Meissner, S., Tabuchi, A., Mertens, M., Kuebler, W. M., and Koch, E., "Virtual four-dimensional imaging of lung parenchyma by optical coherence tomography in mice.," *Journal of biomedical optics* **15**(3), 036016 (2010).

[13] Hanna, N., Saltzman, D., Mukai, D., Chen, Z., Sasse, S., Milliken, J., Guo, S., Jung, W., Colt, H., and Brenner, M., "Two-dimensional and 3-dimensional optical coherence tomographic imaging of the airway, lung, and pleura.," *The Journal of thoracic and cardiovascular surgery* **129**, 615–623 (Mar. 2005).

[14] Quirk, B. C., McLaughlin, R. a., Curatolo, A., Kirk, R. W., Noble, P. B., and Sampson, D. D., "In situ imaging of lung alveoli with an optical coherence tomography needle probe.," *Journal of biomedical optics* **16**, 036009 (Mar. 2011).

[15] Pitris, C., Brezinski, M. E., Bouma, B. E., Tearney, G. J., Southern, J. F., and Fujimoto, J. G., "High resolution imaging of the upper respiratory tract with optical coherence tomography: a feasibility study.," *American journal of respiratory and critical care medicine* **157**, 1640–1644 (May 1998).

[16] Hsia, C. C. W., Hyde, D. M., Ochs, M., and Weibel, E. R., "An official research policy statement of the american thoracic Society/European respiratory society: Standards for quantitative assessment of lung structure," *American Journal of Respiratory and Critical Care Medicine* **181**, 394–418 (Feb. 2010).

[17] Lorbeer, R.-A., Heidrich, M., Lorbeer, C., Ramírez Ojeda, D. F., Bicker, G., Meyer, H., and Heisterkamp, A., "Highly efficient 3D fluorescence microscopy with a scanning laser optical tomograph," *Optics Express* **19**, 5419–5430 (Mar. 2011).

[18] Sharpe, J., Ahlgren, U., Perry, P., Hill, B., Ross, A., Hecksher-Sørensen, J., Baldock, R., and Davidson, D., "Optical projection tomography as a tool for 3D microscopy and gene expression studies," *Science* **296**, 541 –545 (Apr. 2002).

[19] Heidrich, M., Kühnel, M. P., Kellner, M., Lorbeer, R., Lange, T., Winkel, A., Stiesch, M., Meyer, H., and Heisterkamp, A., "3D imaging of biofilms on implants by detection of scattered light with a scanning laser optical tomograph," *Biomedical Optics Express* **2**, 2982–2994 (Nov. 2011).

[20] Knudsen, L., Ochs, M., MacKay, R., Townsend, P., Deb, R., Mühlfeld, C., Richter, J., Gilbert, F., Hawgood, S., Reid, K., and Clark, H., "Truncated recombinant human SP-D attenuates emphysema and type II cell changes in SP-D deficient mice," *Respiratory Research* **8**(1), 70 (2007). PMID: 17915009 PMCID: PMC2078589.

[21] Knudsen, L., Wucherpfennig, K., Mackay, R.-M., Townsend, P., Mühlfeld, C., Richter, J., Hawgood, S., Reid, K., Clark, H., and Ochs, M., "A recombinant fragment of human surfactant protein d lacking the short collagen-like stalk fails to correct morphological alterations in lungs of SP-D deficient mice," *The Anatomical Record: Advances in Integrative Anatomy and Evolutionary Biology* **292**(2), 183–189 (2009).

[22] Kellner, M., Heidrich, M., Beigel, R., Lorbeer, R., Knudsen, L., Ripken, T., Heisterkamp, A., Meyer, H., Kühnel, M. P., and Ochs, M., "Imaging of the mouse lung with scanning laser optical tomography (SLOT)," *Journal of Applied Physiology* **113**, 975–983 (Sept. 2012).

[23] Spalteholz, W., [*Über das Durchsichtigmachen von menschlichen und tierischen Präparaten und seine theoretischen Bedingungen, nebst Anhang: Über Knochenfärbung.*], S. Hirzel, Leipzig (1911).

[24] Kak, A. C. and Slaney, M., [*Principles of computerized tomographic imaging*], Classics in applied mathematics, Society for Industrial and Applied Mathematics, Philadelphia, Pa. (1988).

[25] Vock, R. and Weibel, E. R., "Massive hemorrhage causes changes in morphometric parameters of lung capillaries and concentration of leukocytes in microvasculature," *Experimental Lung Research* **19**, 559–577 (July 1993).

[26] Freem, L. J., Escot, S., Tannahill, D., Druckenbrod, N. R., Thapar, N., and Burns, A. J., "The intrinsic innervation of the lung is derived from neural crest cells as shown by optical projection tomography in wnt1-Cre;YFP reporter mice," *Journal of Anatomy* **217**(6), 651–664 (2010).

[27] Weibel, E. R., Hsia, C. C. W., and Ochs, M., "How much is there really? why stereology is essential in lung morphometry," *Journal of Applied Physiology* **102**, 459–467 (Jan. 2007).